Thermal Conductivity of Anodic Alumina Film at (220 to 480) K by Laser Flash Technique

An Cai,*,†,‡ Li-ping Yang,† Jiang-ping Chen,‡ Tong-geng Xi,† Shi-gang Xin,† and Wei Wu†

Shanghai Institute of Ceramics, Chinese Academy of Sciences, Shanghai, 200050, China, and Shanghai Jiao Tong University, 800 Dongchuan Road, Shanghai, 200240, China

The thermal conductivity at (220 to 480) K of anodic alumina film of (1.4 to 5) μm thick and about 30 % porosity, which is grown from aluminum foil, is reported. A laser flash technique was employed to carry out measurements of thermal diffusivity of layered anodic aluminum specimen, while the effective thermal conductivity of anodic alumina film was determined using a two-layered model, which is 1.22 $W\cdot m^{-1}\cdot K^{-1}$ at 220 K and 1.71 $W\cdot m^{-1}\cdot K^{-1}$ at 480 K. Agreement in the overlapping temperature range (220 to 300) K with the measurements of Chen is found. The results showed that the thermal conductivity of anodic alumina films has a temperature dependence of amorphous solids, and the apparent thickness dependence of thermal conductivity is not found for anodic alumina films.

Introduction

Anodic alumina film,[1] which is formed on the surface of aluminum by anodic reactions, is a material of technological interest in a number of fields, from photonic crystals[2,3] to biosensors,[4] template-based fabrication of metal nanowires,[5,6] and thermal control coatings.[7] The thermal transport property of this material may be very important in such diverse applications.[8] The result of Ogden et al. [9] showed that the thermal conductivity of thick industrial anodic alumina films on aluminum blocks with thickness of (20 to 120) μm ranged from (0.5 to 1) $W\cdot m^{-1}\cdot K^{-1}$ at room temperature, which departs from bulk values (about 30 $W\cdot m^{-1}\cdot K^{-1}$) by an order of magnitude. Stark[10] reports a thermal conductivity of 1.6 $W\cdot m^{-1}\cdot K^{-1}$ of free-standing amorphous anodic alumina film with a thickness of 140 nm. Borca-Tasciuc and Chen[8] measured a 55 μm thick anodic alumina template from (80 to 300) K, and the thermal conductivity is 1.3 $W\cdot m^{-1}\cdot K^{-1}$ at 300 K. However, thermal properties of anodic alumina films above room temperature are seldom found. The purpose of this paper is to research thermal conductivity of anodic alumina thin films with a thickness ranging from (2 to 5) μm for heat transfer normal to the plane of the film by a laser flash technique in the temperature range of (220 to 480) K.

Experiments

The laser flash technique theory and the general description of the principles of measurement are described by Ohta et al.[11] When a laser pulse with energy Q is instantaneously and homogeneously absorbed by the front specimen surface, the specimen rear face temperature distribution can be given by

$$T(t) = \frac{Q}{\rho C_p L}\left[1 + \sum_{n=1}^{\infty}(-1)^n \exp\left(\frac{-n^2\pi^2}{L^2}\alpha t\right)\right] \qquad (1)$$

Then the maximum temperature is

$$T_{max} = \frac{Q}{\rho C_p L} \qquad (2)$$

Upon the introduction of two nondimensional parameters

$$\theta(t) = \frac{T(t)}{T_{max}} \qquad t' = \frac{\pi^2 \alpha t}{L^2} \qquad (3)$$

The normalized rear surface temperature response is

$$\theta(t') = 1 + \sum_{n=1}^{\infty}(-1)^n \exp(-n^2 t') \qquad (4)$$

where L is the specimen thickness and ρ and C_p are the density and specific heat, respectively.

If we assume $\theta(t') = 0.5$ in eq 4, it results in $t' = 1.37$, and then the thermal diffusivity is calculated by

$$\alpha = \frac{\omega \cdot 1.37 \cdot L^2}{\pi^2 t_{1/2}} \qquad (5)$$

where ω is the Cowan[12] correction factor for heat loss and $t_{1/2}$ is the time needed for the rear face temperature to reach one-half of its maximum rise.

The apparatus is shown schematically in Figure 1. A Q-switched Nd:YAG laser (SLI-10, Continuum, USA) at a wavelength of 1064 nm is used as the laser flash source. The maximum energy of a single pulse is 450 mJ, and the pulse duration time is less than 8 ns. The radiation of the sample's rear surface is focused by an antireflection-coated Ge lens of 27.4 mm in focal length and 28.8 mm in diameter to an infrared detector. To achieve high sensitivity and high speed of response at the low temperature, a liquid nitrogen cooled PV mercury

* Corresponding author. E-mail: caian@mail.sic.ac.cn.
† Shanghai Institute of Ceramics.
‡ Shanghai Jiao Tong University.

10.1021/je100437j
Published on Web 07/06/2010

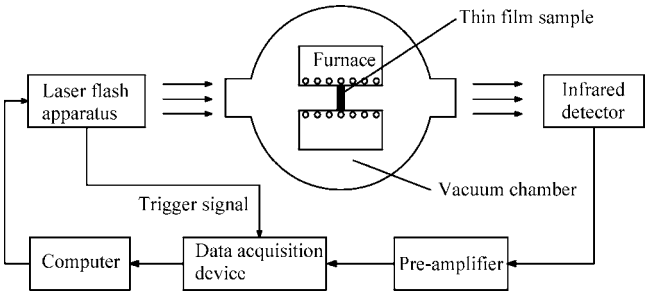

Figure 1. Diagram of the apparatus.

cadmium telluride (MCT) detector of 1.0 mm in diameter (PV-12-1, Fermionics Corp., USA) is used. The photocurrent signal of MCT detector is led into a biased low-noise preamplifier with 10 MHz in bandwidth, and its output is coupled to a digital oscilloscope (TDS3032B, Tek, USA), which is triggered by the external trigger signal of the laser source.

The apparent thermal diffusivity α_e of a two-layed specimen is measured by the apparatus. The two-layered model is described by Araki et al.[13] The mean thermal diffusivity α_m for the two-layered material is expressed as

$$\frac{L}{\alpha_m \rho_m c_m} = \frac{l_1}{\alpha_1 \rho_1 c_1} + \frac{l_2}{\alpha_2 \rho_2 c_2} \tag{6}$$

with the relation of

$$\rho_m L = \rho_1 l_1 + \rho_2 l_2 \qquad c_m \rho_m L = c_1 \rho_1 l_1 + c_2 \rho_2 l_2 \tag{7}$$

where α_1 and α_2 are the thermal diffusivity of alumina film and aluminum substrate, respectively; l_1 and l_2 are the thickness of alumina film and aluminum substrate, respectively; c_1 and c_2 are the specific heat of alumina film and aluminum substrate, respectively; ρ_1 and ρ_2 are the density of alumina film and aluminum substrate, respectively; c_m and ρ_m are specific heat and density of the two-layed specimen, respectively. The apparent thermal diffusivity α_e of a two-layed specimen is a measured value by laser flash technique, and the mean thermal diffusivity α_m of the specimen is a theoretic value defined from thermal resistance by eq 6. The relation between α_e and α_m is

$$\frac{\alpha_m}{\alpha_e} = \frac{4[(A_F - 2A_S) + (1 - A_F + A_S)\eta_{2/1} + A_S \eta_{1/2}]^2}{(1 + H_{2/1}) + \eta_{2/1}^2 (1 + H_{1/2})} \tag{8}$$

With the relation of

$$\eta_i = \frac{l_i}{\sqrt{\alpha_i}} \quad \eta_{i/j} = \frac{\eta_i}{\eta_j} \quad \Lambda_i = \frac{\lambda_i}{\sqrt{\alpha_i}} \quad \Lambda_{i/j} = \frac{\Lambda_i}{\Lambda_j} \quad H_i = \Lambda_i \eta_i \times$$
$$\kappa = \frac{\Lambda_{1/2}}{1 + \Lambda_{1/2}} \quad A_F = 0.5 - 0.3592(\kappa - 0.5) \times$$
$$A_S = 0.3572(\kappa - 0.5)^2 \quad H_{i/j} = \frac{H_i}{H_j} \quad (i,j = 1, 2) \tag{9}$$

The parameters of aluminum for calculation are from the TPRC data serial manual.[14] Then thermal conductivity κ of anodic alumina film is obtained by

$$\kappa = \alpha_1 \rho_1 c_1 \tag{10}$$

Results and Discussion

Verification of Apparatus. Nickel foil with 44 μm in thickness is measured to check the performance of the apparatus. The Ni film sample is well-annealed high-purity nickel having the residual electrical resistivity of 0.0112 $\mu\Omega\cdot$cm. The measured thermal diffusivities agree well with recommended values of TPRC,[14] and the largest deviation is -3 % (Figure 2).

Anodic Alumina Films. The aluminum foil is 50 μm thick (grade LO_3, mass fraction of Al is 0.9999) and is annealed in muffle furnace at 500 °C for 2 h. Then the foil is cleaned by ultrasound in acetone, ethanol, and deionized water. Alumina thin films with a thickness of (1.4, 2.5, and 5) μm are directly grown from the foil in sulfuric acid electrolyte when the condition is that the voltage is 25 V, the concentration of sulfuric acid is 0.3 mol$\cdot$L^{-1}, and the time is (1, 2, and 3) h. The thickness is determined by TaylorStep. The thickness gauge is verified by scanning electron microscopy (SEM). The SEM of the surface and cross-section of anodic alumina film with a thickness of 1.4 μm is shown in Figures 3 and 4. The film has an amorphous structure, and the pore diameter is ~30 nm. The EDS spectrum shows that the film is composed of pure alumina. Its thickness is measured in 10 different consecutive places, and the relative uncertainty of thickness measurement is estimated as 3 %. The thickness in eq 8 is quadratic term, and the thickness uncertainty should multiply by 2. The final relative uncertainty combines thickness uncertainty and random uncertainty of apparent thermal diffusivity measurement of 3 % and gives 9 %.

Temperature Dependence of Thermal Conductivity. The mean thermal diffusivity of the two-layered aluminum foil was

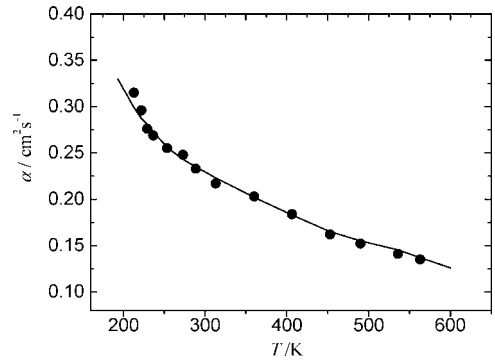

Figure 2. Temperature dependence of thermal diffusivities experimental values and recommended values of Ni foil with thickness of 44 μm. Full line denotes TPRC recommended values; ● denotes experimental values.

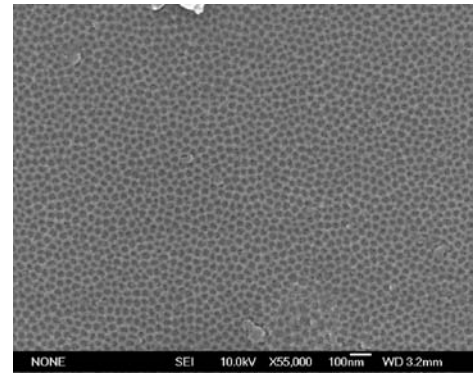

Figure 3. SEM image of the surface of anodic alumina film.

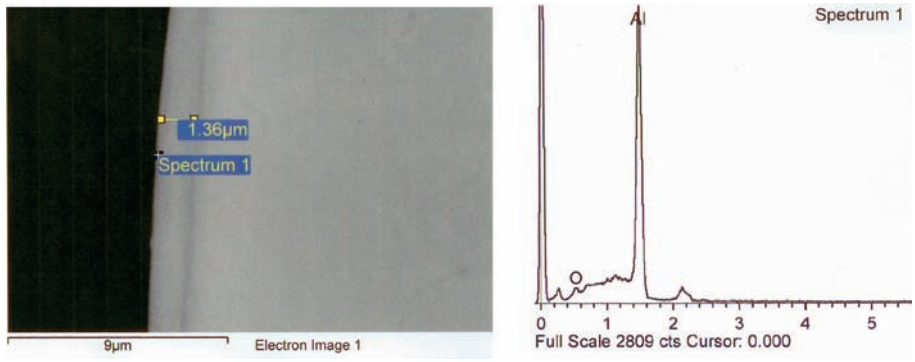

Figure 4. SEM and EDS results of the cross-section of anodic alumina film.

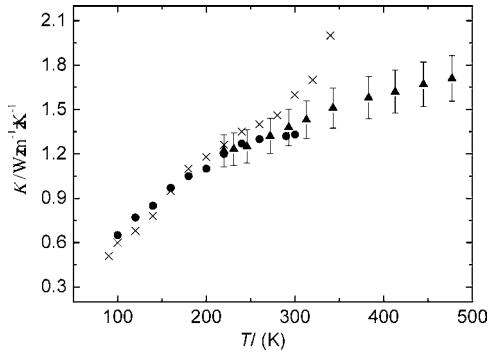

Figure 5. Effective thermal conductivity K along the growth direction (▲, this work, with error bars representing a relative uncertainty of 9 %) of anodic alumina film of (1.4 to 5) μm thickness and ~30 % porosity. Also shown for comparison is K of 140 nm anodic alumina film (×, ref 10 by Stark et al.) and K of amorphous alumina templates of ~30 % porosity and 0.02 μm pore diameter (●, ref 8 by Chen and Borca-Tasciuc).

measured by the apparatus, and then thermal diffusivity and thermal conductivity of anodic alumina film were determined by the two-layered model[13] with thermal properties of Al in room temperature as $\rho_2 = 2.70\ \mathrm{g \cdot cm^{-3}}$, $c_2 = 0.88\ \mathrm{J \cdot g^{-1} \cdot K^{-1}}$, and $\alpha_2 = 0.970\ \mathrm{cm^2 \cdot s^{-1}}$ from TPRC data serials; the porosity of the alumina film was about 30 %. The anodic alumina film is grown from the foil, and there is no apparent boundary between the film and the foil, so thermal boundary resistance between the film and the foil is neglected in this paper. The thermal conductivity of film with a thickness of 2.5 μm between (220 and 480) K is plotted in Figure 5. In the overlapping temperature range (220 to 300) K, our results agree well with the measurements of Chen.[8] This can be explained in two ways. First, Stark uses the steady state method to measure thermal conductivity, and it has a larger uncertainty around room temperature than the 3ω method and photothermoelectric technique, which are employed to determine thermal conductivity of films by Chen.

Second, the expression for thermal conductivity of dielectric solids is

$$\kappa = C_v V l \qquad (11)$$

where C_v is the specific heat, V is the Debye sound velocity, and l is an average phonon mean free path. For amorphous solids l is in the order of the intermolecular spacing and independent of the temperature[15] above 30 K. This means that the increase of thermal conductivity κ can be qualitatively understood as temperature dependence of specific heat C_v with increasing temperature (see eq 11), which is distinctly different from crystalline ones. Because of the amorphous state of the alumina films, Stark et al.[10] consider the thermal conductivity κ in the frame of the theoretical model of the minimum thermal conductivity of a crystal described by Slack. In the model, the average phonon mean free path is constant in the temperature range, and it is valid for all amorphous materials. The calculated minimum κ rises with increasing temperature, and the rising slope decreases slowly. That temperature dependence can be noted in the thermal conductivity curve of Chen and our measurement. This trend is correct for the κ of alumina film and fits better with the results of Chen and this paper. So the measurement of Chen and this paper is more accurate in the overlapping temperature range (220 to 300) K.

Table 1. Comparison of the Thermal Conductivity (T = 300 K) of Alumina Films

κ/W·m^{-1}·K^{-1}	remarks	ref
0.72	alumina film on silicon by electron beam, (0.5 to 4) μm	10
0.73	thick anodic alumina film, (20 to 100) μm	9
1.6	amorphous anodic alumina film, 0.14 μm	10
1.33	anodic templates, 55 μm	8
1.4	amorphous anodic alumina film, (1.4 to 5) μm	this paper

The apparent thickness dependence for anodic alumina films in the thickness range (1.4 to 5) μm is not observed. The available reference thermal conductivity of alumina films is listed in Table 1. It can be noted that there is not a thickness dependence in others' papers.

Conclusion

This work reports the characterization of thermal properties of anodic alumina films of about 30 nm pore diameter and about 30 % porosity with a thickness of (1.4 to 5) μm at temperatures from (220 to 480) K. Effective thermal conductivity of anodic alumina films are determined using two-layered model, which is 1.22 W·m^{-1}·K^{-1} at 220 K and 1.71 W·m^{-1}·K^{-1} at 480 K. Agreement in the overlapping temperature range (220 to 300) K with the measurements of Chen is found. The results show that the thermal conductivity of anodic alumina films has a temperature dependence of amorphous solids and the apparent thickness dependence of thermal conductivity is not found for anodic alumina films.

Acknowledgment

We are very grateful to Zhou X. Y. for his help in apparatus design and Prof. Xu F. F. for his help in english revision.

Literature Cited

(1) Diggle, J. W.; Downie, T. C.; Goulding, C. W. Anodic oxide films on aluminum. *Chem. Rev.* **1969**, *69*, 365–405.

(2) Li, A. P.; Müller, F.; Birner, A.; Nielsch, K.; Gösele, U. Fabrication and microstructuring of hexagonally ordered two-dimensional nanopore arrays in anodic alumina. *Adv. Mater.* **1999**, *11*, 483–487.
(3) Sauer, G.; Brehm, G.; Schneider, S.; Nielsch, K.; Wehrspohn, R. B.; Choi, J. Highly ordered monocrystallie silver nanowire arrays. *J. Appl. Phys.* **2002**, *91*, 3243–3247.
(4) Stura, E.; Bruzzese, D.; Valerio, F.; Grasso, V.; Perlo, P.; Nicolini, C. Anodic porous alumina as mechanical stability enhancer for LDL-cholesterol sensitive electrodes. *Biosens. Bioelectron.* **2007**, *23*, 655–660.
(5) Li, F.; Metzger, R. M. Activation volume of α-Fe particles in alumite films. *J. Appl. Phys.* **1997**, *81*, 3806–3808.
(6) Sun, M.; Zangari, G.; Metzger, R. M. Cobalt island arrays with in-plane anisotropy electrodeposited in highly ordered alumite. *IEEE Trans. Magn.* **2000**, *36*, 3005–3008.
(7) Sharma, A. K. Surface engineering for thermal control of spacecraft. *Surf. Eng.* **2005**, *21*, 249–253.
(8) Borca-Tasciuc, D. A.; Chen, G. Anisotropic thermal properties of nanochanneled alumina templates. *J. Appl. Phys.* **2005**, *97*, 9.
(9) Ogden, T. R.; Rathsam, A. D.; Gilchrist, J. T. Thermal Conductivity of Thick Anodic Oxide Coatings on Aluminum. *Mater. Lett.* **1987**, *5*, 84–87.
(10) Stark, I.; Stordeur, M.; Syrowatka, F. Thermal-Conductivity of Thin Amorphous Alumina Films. *Thin Solid Films* **1993**, *226*, 185–190.
(11) Ohta, H.; Shibata, H.; Waseda, Y. New Attempt for Measuring Thermal-Diffusivity of Thin-Films by Means of a Laser Flash Method. *Rev. Sci. Instrum.* **1989**, *60*, 317–321.
(12) Cowan, R. D. Pulse method of measuring thermal diffusivity at high temperatures. *J. Appl. Phys.* **1963**, *34*, 926–927.
(13) Araki, N.; Makino, A.; Mihara, J. Measurement and Evaluation of the Thermal-Diffusivity of Two-Layered Materials. *Int. J. Thermophys.* **1992**, *13*, 331–349.
(14) Touloukian, Y. S.; Ho, C. Y. *Thermophysical Properties of Matter Thermal Diffusivity*; Plenum Press: New York, 1973.
(15) Choy, C. L.; Leung, W. P.; Xi, T. G.; Fei, Y.; Shao, C. F. Specific-Heat and Thermal-Diffusivity of Strontium Barium Niobate (Sr1-Xbaxnb2o6) Single-Crystals. *J. Appl. Phys.* **1992**, *71*, 170–173.

Received for review April 28, 2010. Accepted June 24, 2010. This work was supported by National Natural Science Foundation of China (Grant No.: 50706057).

JE100437J